NEOPLASIA
www.neoplasia.com

Volume 14 Number 12 December 2012 pp. 1144–1152 1144

MicroRNA Expression Profiling of Peripheral Blood Samples Predicts Resistance to First-line Sunitinib in Advanced Renal Cell Carcinoma Patients[1,2]

Angelo Gámez-Pozo*, Luis M. Antón-Aparicio†, Cristina Bayona‡,3, Pablo Borrega§,3, María I. Gallegos Sancho¶,3, Rocío García-Domínguez#,3, Teresa de Portugal,3, Manuel Ramos-Vázquez††,3, Ramón Pérez-Carrión‡‡, María V. Bolós§§, Rosario Madero¶¶, Iker Sánchez-Navarro*, Juan A. Fresno Vara* and Enrique Espinosa Arranz*,##**

*Laboratory of Molecular Oncology and Pathology, Instituto de Genética Médica y Molecular (INGEMM), Instituto de Investigación Sanitaria del Hospital Universitario La Paz (IdiPAZ), Madrid, Spain; †Medical Oncology Department, La Coruña University Hospital, Servicio Galego de Saúde (SERGAS), La Coruña, Spain; ‡Oncology Department, Hospital General Yagüe, Burgos, Spain; §Medical Oncology Department, Hospital de San Pedro de Alcántara, Cáceres, Spain; ¶Medical Oncology Department, Hospital General de Segovia, Segovia, Spain; #Medical Oncology Department, Hospital Universitario de Salamanca, Salamanca, Spain; **Medical Oncology Department, Hospital Virgen de la Concha, Complejo Hospitalario de Zamora, Zamora, Spain; ††Medical Oncology Department, Centro Oncológico de Galicia, A Coruña, Spain; ‡‡Oncology Department, Hospital Quirón, Madrid, Spain; §§Pfizer Oncology, Madrid, Spain; ¶¶Statistics Department, Instituto de Investigación Sanitaria del Hospital Universitario La Paz (IdiPAZ), Madrid, Spain; ##Medical Oncology Department, Hospital Universitario La Paz, Madrid, Spain

Abstract

Anti-angiogenic therapy benefits many patients with advanced renal cell carcinoma (RCC), but there is still a need for predictive markers that help in selecting the best therapy for individual patients. MicroRNAs (miRNAs) regulate cancer cell behavior and may be attractive biomarkers for prognosis and prediction of response. Forty-four patients with RCC were recruited into this observational prospective study conducted in nine Spanish institutions. Peripheral blood

Abbreviations: MSKCC, Memorial Sloan-Kettering Cancer Center; RCC, renal cell carcinoma; miRNAs, microRNAs

Address all correspondence to: Enrique Espinosa Arranz, MD, Servicio de Oncología Médica, Hospital de Día 1ª Planta, Instituto de Investigación Sanitaria del Hospital Universitario La Paz (IdiPAZ), Paseo de la Castellana, 261-28046 Madrid, Spain. E-mail: eespinosa00@hotmail.com or Juan Ángel Fresno Vara, PhD, Instituto de Genética Médica y Molecular (INGEMM), Instituto de Investigación Sanitaria del Hospital Universitario La Paz (IdiPAZ), Paseo de la Castellana, 261-28046 Madrid, Spain. E-mail: juanangel.fresno@idipaz.es

[1]This study was supported by an unrestricted educational grant from Pfizer. The funders had no role in study design, data analysis, decision to publish, or preparation of the manuscript. This research was also supported by grants FIS CP05/00248 and Red Temática de Investigación Cooperativa en Cáncer (RTICC, RD06-0020-1022) from Instituto de Salud Carlos III, Ministerio de Ciencia e Innovación, Spain. I.S.-N. is supported by Fundación para la Investigación Biomédica del Hospital Universitario La Paz (FIBHULP). M.V.B. is an employee of Pfizer Oncology in Spain. All other authors state that they have no conflicts of interest for this study. Some results contained in this work were presented as a poster at the European Society for Medical Oncology (ESMO, Stockholm, Sweden; September 2011) and the Sociedad Española de Oncología Médica (SEOM, Málaga, Spain; October 2011).

[2]This article refers to supplementary materials, which are designated by Appendix Materials, Tables W1 to W4 and Figures W1 to W7 and are available online at www.neoplasia.com.

[3]These authors have contributed equally to this manuscript.

Received 27 April 2012; Revised 10 October 2012; Accepted 12 October 2012

DOI 10.1593/neo.12734

samples were taken before initiation of therapy and 14 days later in patients receiving first-line therapy with sunitinib for advanced RCC. miRNA expression in peripheral blood was assessed using microarrays and L2 boosting was applied to filtered miRNA expression data. Several models predicting poor and prolonged response to sunitinib were constructed and evaluated by binary logistic regression. Blood samples from 38 patients and 287 miRNAs were evaluated. Twenty-eight miRNAs of the 287 were related to poor response and 23 of the 287 were related to prolonged response to sunitinib treatment. Predictive models identified populations with differences in the established end points. In the poor response group, median time to progression was 3.5 months and the overall survival was 8.5, whereas in the prolonged response group these values were 24 and 29.5 months, respectively. Ontology analyses pointed out to cancer-related pathways, such angiogenesis and apoptosis. miRNA expression signatures, measured in peripheral blood, may stratify patients with advanced RCC according to their response to first-line therapy with sunitinib, improving diagnostic accuracy. After proper validation, these signatures could be used to tailor therapy in this setting.

Neoplasia (2012) 14, 1144–1152

Introduction

Renal cell carcinoma (RCC) accounts for 3% of all malignant tumors and affects more than 12,000 people every year in the United States [1]. Most patients with localized disease can be cured with surgery, but less than 20% of patients with advanced disease remain alive at 5 years [2,3]. Anti-angiogenic therapy has revolutionized therapy for metastatic disease, so that life expectancy has risen from 13 to 15 months in the year 2002 to 26 months nowadays [4–6]. Available options for first-line therapy include sunitinib [7], pazopanib [8], and the combination of interferon plus bevacizumab [9,10], as well as temsirolimus for poor prognosis patients [11].

Although most patients benefit from new drugs, some still have early progression [11–29% of patients treated with vascular endothelial growth factor (VEGF) target therapy exhibit progressive disease (PD) as best response] and suffer unnecessary toxicity. For this reason, recent studies have focused on the identification of factors that predict drug response [12,13]. These studies have analyzed a limited number of markers and their results can be considered preliminary, so further refinement is needed in the field.

MicroRNAs (miRNAs) are a class of small noncoding RNAs that control gene expression by targeting mRNA [14]. miRNAs play an important role as regulators of gene expression in tumorigenesis by controlling many biologic processes in growth, development, differentiation, and apoptosis. miRNA expression profiles have been suggested as a promising new class of biomarkers for tumor diagnosis [15–17], prognosis [18], and prediction of response to different drugs [19]. Predictive markers are particularly interesting to optimize therapy. In the present study, we assessed miRNA expression in peripheral blood of patients receiving sunitinib for advanced RCC, estimating diagnostic accuracy of these miRNAs in the prediction of sunitinib response.

Materials and Methods

Patient Selection

Eligible patients were 18 years old or above, with a pathologically confirmed diagnosis of RCC, having locally or distant advanced disease who has not received any systemic treatment for kidney cancer, including cytokines, and who were scheduled for sunitinib in a daily practice setting. Peripheral blood samples were taken before initiation of therapy and 2 weeks later. Eligible patients should remain at least 14 days on therapy to be considered for analysis. This study was approved by an Institutional Ethics Review Board, and written and signed consent was obtained in all cases.

Study Design

Patients were prospectively entered into this multiinstitutional SUT-IIG9 study performed in nine Spanish Hospitals. Drug schedule, policy for dose reductions or dose delay, and timing for radiologic assessments were made in accordance with current, local practice guidelines. Demographic and clinical data were recorded on specific case record forms and periodically reviewed by an external monitor. Samples were anonymized and molecular analysis was performed blinded to clinical data. Study recruitment started on 26 November 2007 and finished on 17 September 2010, and the database was closed for follow-up on 17 May 2011. The authors designed the study, analyzed and held the data, wrote the manuscript, made the decision to submit the manuscript for publication, and vouch for the accuracy and completeness of the data and analyses. Prospective diagnostic study was according to Standards for Reporting of Diagnostic Accuracy guidelines.

Total RNA Extraction

Leukocytes were captured using the LeukoLOCK System and stabilized using RNA*later* (Ambion, Life Technologies, Carlsbad, CA). Total RNA was extracted with the miRNeasy Mini Kit (Qiagen, Hilden, Germany) following the manufacturer's protocol. Purified RNA quality control for quantity and purity was assessed using an ND-1000 NanoDrop spectrophotometer (NanoDrop Technologies, Wilmington, DE).

miRNA Arrays

Samples were hybridized to Human miRNA Microarray Release 14.0, 8x15K (Agilent Technologies, Santa Clara, CA). MicroRNA Labeling Kit (Agilent Technologies) was used to label RNA. Basically, 100 ng of total RNA was dephosphorylated and cyanine 3–cytidine biphosphate (pCp) molecule was ligated to the 3′ end of each RNA molecule by using T4 RNA ligase. One hundred nanograms of cyanine 3–labeled RNA was hybridized for 20 hours at 55°C in a hybridization

oven (G2545A; Agilent Technologies) set to 20 rpm in a final concentration of 1× GE blocking agent and 1× Hi-RPM hybridization buffer, according to the manufacturer's instructions (miRNA Microarray System Protocol; Agilent Technologies). Arrays were washed according to the manufacturer's instructions (miRNA Microarray System Protocol; Agilent Technologies), dried out using a centrifuge at 1000 rpm for 2 minutes, and scanned at 5-μm resolution on an Agilent DNA Microarray Scanner (G2565BA; Agilent Technologies) equipped with extended dynamic range (XDR) software. Images provided by the scanner were analyzed using Agilent's software Feature Extraction version 10.7.3.1. Data were normalized using Variance Stabilization Normalization [20]. Only miRNAs with an average intensity over the 20th percentile of the overall intensities, a detectable signal in at least 15 of the 76 samples hybridized, and a normalized mean expression of more than 0.9 were considered for further analysis.

Predictive Models

Predictive models were built independently for poor response and prolonged response. L2 boosting for classification with classic Akaike information criterion (AIC) based on the binomial log likelihood for stopping the boosting iteration algorithm was applied to filtered miRNA expression data obtained from basal blood samples [21] to identify variables related to clinical information. Twelve predictive models for one, two, three, or four variables were built using a binary logistic regression with the Fisher scoring as an optimization technique. Predictive accuracy for calibration was assessed by the Hosmer-Lemeshow test [22]. Discriminant power was evaluated by area under the receiver operating characteristic (ROC) curve (AUC) of data training and leave-one-out cross-validated (LOOCV) ROC curves and C index [23]. A cutoff of 0 was used for every model. A subgroup analysis according to Memorial Sloan-Kettering Cancer Center (MSKCC) prognostic scale was performed. One point was assigned for diagnosis-to-treatment interval < 1 year, Karnofsky performance status (KPS) < 80, low hemoglobin, elevated serum calcium, elevated lactate dehydrogenase (LDH) 1.5 times the upper limit of normal; zero points constituting the favorable prognosis group, one or two points the intermediate prognosis group, and three or more points the poor prognosis group [24].

Statistical Analyses

We defined progression-free survival (PFS) as the time between the first day of treatment with sunitinib and the date of radiologic PD, clear clinical evidence of PD, or death. Patients who had not progressed at database closure were censored at final follow-up. If the date of PD was unknown, we censored PFS at the last tumor assessment. Overall survival (OS) was defined as the time between the first day of sunitinib treatment and the date of death or last date of follow-up. Objective response was assessed by physicians, according to response evaluation criteria in solid tumors (RECIST), and classified as complete response, partial response, stable disease, or PD. Normalized expression values and fold change values were assessed by nonparametric tests: the Wilcoxon test to compare two paired groups, the Mann-Whitney test to compare two unpaired groups, and the Kruskall-Wallis test to compare three unmatched groups. Survival curves were estimated using Kaplan-Meier analysis and compared using the log-rank test. The primary end point was time to disease progression, defined as the time from start of therapy until the time of documented radiologic progression of the disease, clear clinical progression of the disease, or death from cancer. OS was calculated from the start of therapy until the date of death or last follow-up. All statistical analyses were performed using SAS 9.1 and R(4) with "rdesign" and "mboost" packages. The relationship between OS, the MSKCC prognostic profile, and the poor response models was analyzed using the log-rank test and the Cox proportional hazards model. All tests were two-sided.

Model Validation Using Reverse Transcription–Quantitative Polymerase Chain Reaction

Expressions from miRNAs included in poor response model 3.3 and prolonged response model 3.2 were evaluated using reverse transcription–quantitative polymerase chain reaction (RT-qPCR). cDNA synthesis and real-time qPCR of miR-192, miR-193a-5p, miR-501-3p, miR-410, miR-1181, and miR-424 were performed using the miRCURY LNA Universal RT microRNA PCR system (Exiqon, Vedbaek, Denmark) according to the manufacturer's instructions. The cDNA

Table 1. Clinical Data.

	Number of Patients (%)
Gender	
Men	27 (71)
Women	11 (29)
Age	
Range	47–86
Median	66
Histologic subtype	
Clear cell carcinoma	27 (71)
Papillary	4 (10)
Other	7 (19)
Metastasis location	
Lung	23 (61)
Bone	11 (29)
Lymph nodes	17 (45)
Other	13 (34)
Best response	
Complete	7 (19)
Partial	10 (26)
Stable	10 (26)
Progression	11 (29)
MSKCC prognostic criteria	
Good	3 (8)
Intermediate	26 (68)
Bad	9 (24)
ECOG performance status	
0	21 (55)
1	13 (34)
2	3 (8)
ND	1 (3)
Prior nephrectomy	
Yes	28 (74)
No	10 (26)
Time from diagnosis to treatment	
≥1 year	14 (37)
<1 year	24 (63)
No. of metastatic sites	
≤1	14 (37)
<2	16 (42)
≥3	8 (21)
Hemoglobin	
≥LLN	19 (50)
<LLN	18 (47)
ND	1 (3)
LDH	
≤1.5 × ULN	23 (60)
>1.5 × ULN	14 (37)
ND	1 (3)
Corrected calcium (mg/dl)	
≤10	30 (78)
>10	4 (11)
ND	4 (11)

ECOG, Eastern Cooperative Oncology Group; LLN, lower limit of normal; LDH, lactate dehydrogenase; ULN, upper limit of normal; ND, not described.

products were subsequently diluted 80-fold, and 4 μl was used in 10 μl of PCR reactions and quantified using SYBR Green–based real-time PCR and individual miRNA LNA primer sets. The qPCRs were run on a 7900HT thermocycler (ABI; Applied Biosystems, Life Technologies, Carlsbad, CA) using the thermal cycling parameters recommended by Exiqon. Raw C_t values were calculated as recommended by Exiqon using the RQ manager software v1.2.1 (ABI) with manual settings for threshold and baseline. Relative expression level of each target gene was expressed as $\Delta Cq = Cq_{ref} - Cq_{target}$. Normalization was performed using the mean expression value of two housekeeping miRNAs (mi-103 and miR-191). As predictive models for poor response and prolonged response were defined using microarrays, normalized gene Cq values were *z*-score transformed and scaled as previously described [25].

Analysis of miRNA Targets

Validated targets of miRNAs related with sunitinib response were evaluated using the Validated Target module of miRWalk [26]. Gene ontology analyses including pathways, biologic process, and molecular functions of identified genes were performed in PANTHER [27,28]. miRNA expression in kidney samples was assessed using available data [29].

This work fulfills the Standards for Reporting of Diagnostic Accuracy recommendations.

Results

At the moment of the molecular analysis, 44 consecutive patients were included in the study. Two of them were lost to follow-up without response evaluation, three did not have the second blood sample, and one died before receiving the study drug. Table 1 provides clinical data of the remaining 38 patients. Twelve patients had a progression before 6 months and constitute the poor response group; 10 patients did not have a progression in the first 18 months and were included in the prolonged response group, whereas 16 patients were allocated to the moderate response group. Cutoff point at 6 months was chosen because this was the median time to progression of the control group in the pivotal phase III trial of sunitinib [6].

miRNAs Related with Response to Sunitinib Treatment

Peripheral blood samples obtained before initiation of therapy with sunitinib and 14 days later were used to assess expression values of miRNAs. After data filtering, 287 of 939 miRNAs were considered for subsequent analysis. The data discussed in this publication have been deposited in the National Center for Biotechnology Information's Gene Expression Omnibus and are accessible through Gene Expression Omnibus Series accession number GSE32099 [30]. Comparison of the poor response and response groups found significant differences in the expressions of 28 miRNAs of the 287 evaluated when L2 boosting was applied to filtered miRNA expression data obtained from basal blood. Additionally, L2 boosting identified 28 variables related to prolonged response to sunitinib. Fourteen of these variables corresponded to miRNAs found in the basal blood samples, four of them were detected in day 14 blood samples, and the remaining 10 variables corresponded to significant changes in miRNA expression between basal and day 14 samples (Table 3).

Predictive Models for Poor Response to Sunitinib

Twelve predictive signatures of poor response to sunitinib were built using a binary logistic procedure. The Hosmer-Lemeshow test showed adequate calibration accuracy for all signatures. Discriminant power

Table 2. Twenty-eight miRNAs Related to Response of Sunitinib, Identified by L2 Boosting from the 287 miRNA Basal Expression Values Evaluated.

miRNA	Boosting Coefficient	4.1	4.2	4.3	3.1	3.2	3.3	2.1	2.2	2.3	1.1	1.2	1.3
hiv1-miR-H1	0.0181												
hsa-miR-125a-5p	0.0167				x								
hsa-miR-1308	−0.0385												
hsa-miR-139-3p	0.0343											x	
hsa-miR-141	0.0195												
hsa-miR-145	0.0133												
hsa-miR-150	0.0173												
hsa-miR-181a*	−0.0703	x	x	x		x				x			
hsa-miR-1825	−0.0988												
hsa-miR-192	−0.0045			x			x		x				
hsa-miR-193a-3p	−0.0279						x						
hsa-miR-193a-5p	−0.0558												
hsa-miR-199a-5p	−0.0565												
hsa-miR-29a	0.0196												
hsa-miR-30b*	0.0743									x			
hsa-miR-31	0.0060												
hsa-miR-34a	−0.0531	x	x										
hsa-miR-362-3p	0.0105	x	x										
hsa-miR-370	0.0138												
hsa-miR-501-3p	0.0554			x	x	x	x	x	x				x
hsa-miR-505*	−0.1370				x	x		x					
hsa-miR-516a-5p	0.0369		x								x		
hsa-miR-564	0.0089	x											
hsa-miR-582-5p	0.0037			x									
hsa-miR-624*	−0.0043												
hsa-miR-629	−0.0017												
hsa-miR-659	0.0184												
hsa-miR-933	0.0443												

Twelve predictive models were established; x indicates that miRNA is included in the model.

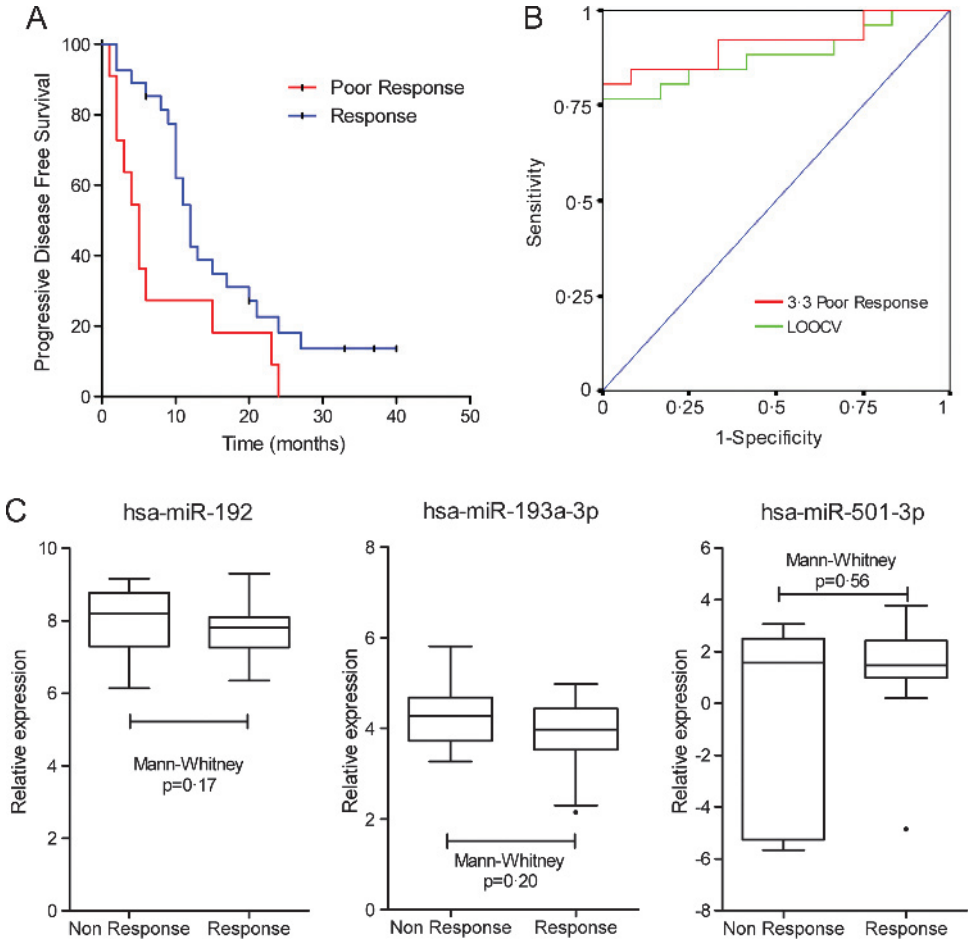

Figure 1. (A) Kaplan-Meier analyses, (B) ROC curves for model and LOOCV, and (C) expression of miRNAs included in the poor response model 3.3.

of the predictive signatures was assessed using different criteria (Figure W1). Complete analyses can be found in the Supplementary Materials. Signatures with two or more miRNAs had better discriminative power than single mRNAs. Table 2 shows the miRNAs included in each predictor. Figure 1 displays expression values of some miRNAs included in models that predicted a poor response to sunitinib. Six-month PFS was 85% for patients included in the response group by, at least, four signatures and 20% for patients in the poor response group (Figure 1 and Tables 3 and W1). In the poor response group, median time to progression was 3.5 months and the OS was 8.5 months, whereas in the prolonged response group these values were 14 and 24 months, respectively.

Predictive Models for Prolonged Response to Sunitinib

Twelve predictive signatures of prolonged response to sunitinib were built. Models with more than one miRNA harbor more discriminative power than just one miRNA (Figure W2). Complete analyses can be found in the Supplementary Materials. Figure 2 displays expression values of some miRNAs included in models that predicted a prolonged response. Eighteen-month PFS was 90% for patients included in the prolonged response group by, at least, five signatures and 6.67% for patients in the moderate response group (Figure 2 and Table W1). In the moderate response group, median time to progression was 11 months and the OS was 23 months, whereas in the prolonged response group these values were 24 and 29.5 months, respectively.

Predictive Model Validation

Expressions from miRNAs included in poor response model 3.3 and prolonged response model 3.2 were evaluated using RT-qPCR in 37 of 38 patients with available RNA (Table W4). Despite platform change (from microarrays to RT-qPCR), both poor response model 3.3 and prolonged response model 3.2 still harbor predictive power (Figure W7).

OS Prediction

MSKCC prognostic scale was calculated for each patient [31]. The proportion of patients in the favorable, intermediate, and poor groups was 8%, 68%, and 24%, respectively. There were no statistical differences in OS between the groups (P = .972). There was no relation between the MSKCC prognosis profile and OS in the univariate analysis (P = .935). Poor response model 3.3, which showed best statistical significance, assigned 11 and 27 patients to the poor response and response groups, respectively. Hazard ratio (HR) between groups was 0.385 [95% confidence interval (95%CI) = 0.161–0.963, P = .032]. The multivariate analysis demonstrated that the poor response model 3.3 was related to OS (HR = 0.463, IC95 = 0.219–0.979, P = .044) but not the MSKCC prognostic profile (P = .897).

Gene Ontology and Metadata Analyses

An overview of genes regulated by miRNAs included in poor response and prolonged response models was obtained using the Validated Target module of miRWalk (Table W2). Gene ontology analyses of these genes were performed using PANTHER database. Most genes target cancer-related pathways such as angiogenesis, p53, Ras, PDGF, apoptosis, and so on (Figure W3). There is also an increased presence of metabolism and signal transduction–related genes (Table W3, online only). Poor response model 3.3 miRNAs (miR-192, miR-193a-5p, miR-501-3p) and prolonged response model 3.2 miRNAs (miR-410 before treatment and miR-1181 and miR-424* fold change) target genes related with KEGG Renal Cell Carcinoma pathway (Figures W4 and W5 and Table W2). The presence of miR-192 and miR-193-5p in normal and tumor kidney samples was confirmed using previously available data (Figure W6) [29].

Discussion

In the present study, the expression of miRNA in the peripheral blood of patients receiving sunitinib for advanced RCC was explored. We combined expression values of several miRNAs to build models related to poor response (progression before 6 months) or prolonged response (progression after 18 months) to this drug. The poor response group is particularly relevant from the clinical point of view, because it might help in identifying patients to whom alternative or even experimental therapies should be offered.

Most promising models were validated using RT-qPCR. Despite the platform change (from microarrays to qPCR), both poor response 3.3 and prolonged response 3.2 models maintained predictive power (Figure W7). This is remarkable, as long as low inter-platform reproducibility among different miRNA platforms has been previously reported [32].

Previous studies have found markers that predict a response to sunitinib in patients with advanced RCC. Hypertension is associated with improved outcome [33], whereas the presence of bone metastases or high tumor burden has a negative impact on survival [34,35]. Some studies have focused on molecular biomarkers of response. For instance, strong expression of VEGF receptor 2 is associated with increased PFS [36], and serum levels of VEGF are related to PD and OS prognosis [37–39]. Other markers such as the level of circulating bone marrow–derived progenitor cells [40], the number of circulating endothelial cells [41], and the levels of brain natriuretic peptide, apolipoprotein A2 (ApoA2), and serum amyloid alpha (SSA) have been reported to affect the outcome in this population [42]. Finally, polymorphisms in *CYP3A5*, *NR113*, and *ABCB1* (genes affecting the pharmacokinetics of sunitinib) are associated with PFS [43].

Information about the role of miRNAs is more limited in this field. A number of studies link miRNAs with cancer, as they regulate transcription factors and can eventually alter apoptosis, cell cycle, and cell migration [15]. miRNA expression patterns vary between clear cell carcinoma and normal kidney [15–17,44], among tumors of different anatomic location and also among multiple tumor subtypes within a single location [45]. miRNA patterns can distinguish between renal cancer subtypes [46] and have been found to correlate with prognosis in patients with RCC [45,47]. It has been suggested that miRNA-106b might be used to predict early metastasis after nephrectomy [48]. With regard to sunitinib, the drug has effects on miRNA expression in mice models [49].

There are previous studies of gene expression [50,51] and miRNA [52] profiling in peripheral blood of patients with RCC. Our study is

Table 3. Twenty-eight Variables Related to Prolonged Response to Sunitinib Treatment Identified by L2 Boosting from 287 miRNA Basal Expression, miRNA after Treatment Expression, and miRNA Fold Change.

miRNA	Sample	Boosting Coefficient	4.1	4.2	4.3	3.1	3.2	3.3	2.1	2.2	2.3	1.1	1.2	1.3
hsa-miR-1228	Basal	−0.1594									x	x		
hsa-miR-1267	Basal	0.0136												
hsa-miR-1290	Basal	−0.1408				x				x				
hsa-miR-136	Basal	0.0635		x				x						
hsa-miR-199a-3p	Basal	−0.0248												
hsa-miR-199a-5p	Basal	−0.0033												
hsa-miR-221	Basal	−0.0999						x						
hsa-miR-31	Basal	0.0336						x						
hsa-miR-34a	Basal	−0.0877		x					x					
hsa-miR-371-5p	Basal	0.0060												
hsa-miR-376a	Basal	0.0037							x					
hsa-miR-410	Basal	0.0277	x		x		x							
hsa-miR-659	Basal	0.0112												
hsa-miR-923	Basal	−0.0263												
hsa-miR-1274a	After	−0.0262		x	x						x			
hsa-miR-193a-5p	After	−0.0542												
hsa-miR-31	After	0.0360		x										
hsa-miR-99b	After	−0.0173												
hsa-miR-1181	Change	−0.0227	x		x	x	x							
hsa-miR-126*	Change	−0.0136	x											
hsa-miR-1267	Change	0.0015												
hsa-miR-193a-5p	Change	0.0037	x											
hsa-miR-198	Change	−0.0250												x
hsa-miR-410	Change	0.0053												
hsa-miR-424*	Change	−0.0367			x	x	x			x			x	
hsa-miR-564	Change	−0.0061												
hsa-miR-630	Change	−0.0054												
hsa-miR-659	Change	0.0036												

Twelve predictive models were established; x indicates that miRNA is included in the model.

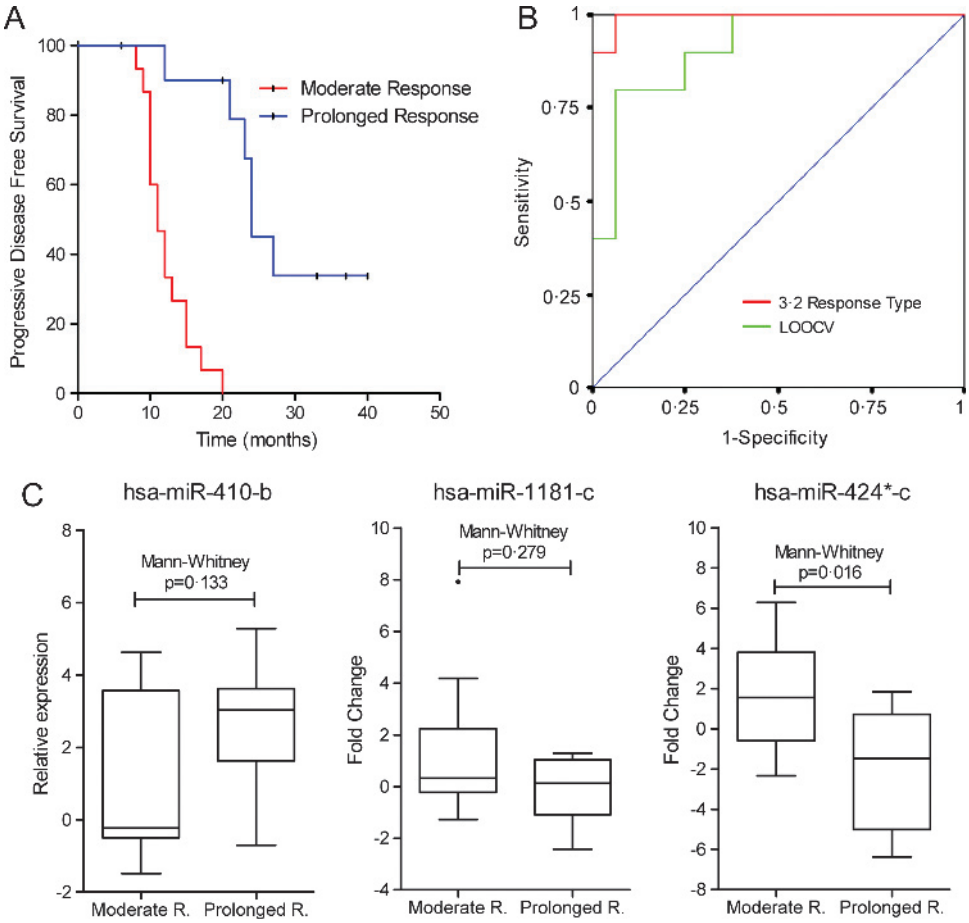

Figure 2. (A) Kaplan-Meier analyses, (B) ROC curves for model and LOOCV, and (C) expression of miRNAs included in the prolonged response model 3.2. b indicates miRNA basal expression. c indicates fold change between basal and day 14 samples.

the first that assess the expression of miRNAs in this tissue to predict response to sunitinib. Although we did not assess the expression of these miRNAs in primary tumors, some of them are detectable in both normal and tumor kidneys according to the literature (Figure W6) [29].

Taken together, the aberrant expression of the miRNAs in the peripheral lymphocytes or monocytes of advanced RCC patients could, to some extent, reflect the sensitivity to sunitinib therapy, which is compatible with the predicted canonical pathways for these miRNAs, including angiogenesis, apoptosis, p53, Ras, and so on. Additionally, some of the targeted genes are directly related with the genesis and development of RCC (Figures W4 and W5). In any case, more studies are needed to elucidate if changes in peripheral blood miRNA expression have any relation with tumor susceptibility or simply reflect host features affecting drug efficacy.

Our predictive model was also related to OS, which could be expected considering that patients with no response to first-line therapy have very limited therapeutic options. The MSKCC prognostic scale did not detect OS differences in our population, as it has been shown previously [53], because most patients had a good performance status, which is a major determinant of prognosis.

Limited size is an obvious limitation in our series, which could have led to model overfitting. Moreover, an independent validation is needed, because miRNAs may vary depending on the population used for the discovery phase. Regardless of these limitations, our point was to demonstrate that a small subset of miRNAs could be informative in peripheral blood. miRNA field is under development, so significant advances are likely to happen in the near future.

Considering the number of available options, treatment recommendations for advanced RCC must be adapted and tailored to each individual patient. Peripheral blood offers a noninvasive alternative to assess predictive markers. miRNA expression profiling in peripheral blood may identify patients that will not benefit from sunitinib therapy before treatment. These patients should receive an alternative fist-line therapy or even be included in clinical trials. However, miRNA expression profiling identified patients with moderate benefit of sunitinib therapy. This population is suitable to explore new therapeutic combinations including sunitinib.

In conclusion, peripheral blood miRNA signatures could be employed to personalize therapy for advanced RCC, both in the selection of existing drugs and in the development of new drugs.

Acknowledgments

We thank Julia Llinares for her contribution to data monitoring and collection, Ana Dopazo and Alberto Benguría (Genomics Unit, Centro Nacional de Investigaciones Cardiovasculares) for their technical support in microarray analyses, Fátima Sánchez Cabo (Bioinformatics Unit, Centro Nacional de Investigaciones Cardiovasculares) for Variance Stabilization Normalization of microarray data, and Rocío López, Esther Díaz, and María Miguel-Martín for technical support.

References

[1] Cohen HT and McGovern FJ (2005). Renal-cell carcinoma. *N Engl J Med* **353**, 2477–2490.

[2] Flanigan RC, Mickisch G, Sylvester R, Tangen C, Van Poppel H, and Crawford ED (2004). Cytoreductive nephrectomy in patients with metastatic renal cancer: a combined analysis. *J Urol* **171**, 1071–1076.

[3] Kavolius JP, Mastorakos DP, Pavlovich C, Russo P, Burt ME, and Brady MS (1998). Resection of metastatic renal cell carcinoma. *J Clin Oncol* **16**, 2261–2266.

[4] Motzer RJ, Bacik J, Murphy BA, Russo P, and Mazumdar M (2002). Interferon-alfa as a comparative treatment for clinical trials of new therapies against advanced renal cell carcinoma. *J Clin Oncol* **20**, 289–296.

[5] Negrier S, Escudier B, Gomez F, Douillard JY, Ravaud A, Chevreau C, Buclon M, Perol D, and Lasset C (2002). Prognostic factors of survival and rapid progression in 782 patients with metastatic renal carcinomas treated by cytokines: a report from the Groupe Français d'Immunothérapie. *Ann Oncol* **13**, 1460–1468.

[6] Motzer RJ, Hutson TE, Tomczak P, Michaelson MD, Bukowski RM, Oudard S, Negrier S, Szczylik C, Pili R, Bjarnason GA, et al. (2009). Overall survival and updated results for sunitinib compared with interferon alfa in patients with metastatic renal cell carcinoma. *J Clin Oncol* **27**, 3584–3590.

[7] Motzer RJ, Hutson TE, Tomczak P, Michaelson MD, Bukowski RM, Rixe O, Oudard S, Negrier S, Szczylik C, Kim ST, et al. (2007). Sunitinib versus interferon alfa in metastatic renal-cell carcinoma. *N Engl J Med* **356**, 115–124.

[8] Sternberg CN, Davis ID, Mardiak J, Szczylik C, Lee E, Wagstaff J, Barrios CH, Salman P, Gladkov OA, Kavina A, et al. (2010). Pazopanib in locally advanced or metastatic renal cell carcinoma: results of a randomized phase III trial. *J Clin Oncol* **28**, 1061–1068.

[9] Escudier B, Pluzanska A, Koralewski P, Ravaud A, Bracarda S, Szczylik C, Chevreau C, Filipek M, Melichar B, Bajetta E, et al. (2007). Bevacizumab plus interferon alfa-2a for treatment of metastatic renal cell carcinoma: a randomised, double-blind phase III trial. *Lancet* **370**, 2103–2111.

[10] Rini BI, Halabi S, Rosenberg JE, Stadler WM, Vaena DA, Ou SS, Archer L, Atkins JN, Picus J, Czaykowski P, et al. (2008). Bevacizumab plus interferon alfa compared with interferon alfa monotherapy in patients with metastatic renal cell carcinoma: CALGB 90206. *J Clin Oncol* **26**, 5422–5428.

[11] Hudes G, Carducci M, Tomczak P, Dutcher J, Figlin R, Kapoor A, Staroslawska E, Sosman J, McDermott D, Bodrogi I, et al. (2007). Temsirolimus, interferon alfa, or both for advanced renal-cell carcinoma. *N Engl J Med* **356**, 2271–2281.

[12] Jain RK, Duda DG, Willett CG, Sahani DV, Zhu AX, Loeffler JS, Batchelor TT, and Sorensen AG (2009). Biomarkers of response and resistance to antiangiogenic therapy. *Nat Rev Clin Oncol* **6**, 327–338.

[13] Tonini G, Fratto ME, Imperatori M, Pantano F, Vincenzi B, and Santini D (2011). Predictive factors of response to treatment in patients with metastatic renal cell carcinoma: new evidence. *Expert Rev Anticancer Ther* **11**, 921–930.

[14] Iorio MV and Croce CM (2009). MicroRNAs in cancer: small molecules with a huge impact. *J Clin Oncol* **27**, 5848–5856.

[15] Chow TF, Youssef YM, Lianidou E, Romaschin AD, Honey RJ, Stewart R, Pace KT, and Yousef GM (2010). Differential expression profiling of microRNAs and their potential involvement in renal cell carcinoma pathogenesis. *Clin Biochem* **43**, 150–158.

[16] Gottardo F, Liu CG, Ferracin M, Calin GA, Fassan M, Bassi P, Sevignani C, Byrne D, Negrini M, Pagano F, et al. (2007). Micro-RNA profiling in kidney and bladder cancers. *Urol Oncol* **25**, 387–392.

[17] Jung M, Mollenkopf HJ, Grimm C, Wagner I, Albrecht M, Waller T, Pilarsky C, Johannsen M, Stephan C, Lehrach H, et al. (2009). MicroRNA profiling of clear cell renal cell cancer identifies a robust signature to define renal malignancy. *J Cell Mol Med* **13**, 3918–3928.

[18] Heinzelmann J, Henning B, Sanjmyatav J, Posorski N, Steiner T, Wunderlich H, Gajda MR, and Junker K (2011). Specific miRNA signatures are associated with metastasis and poor prognosis in clear cell renal cell carcinoma. *World J Urol* **29**, 367–373.

[19] Flamant S, Ritchie W, Guilhot J, Holst J, Bonnet ML, Chomel JC, Guilhot F, Turhan AG, and Rasko JE (2010). Micro-RNA response to imatinib mesylate in patients with chronic myeloid leukemia. *Haematologica* **95**, 1325–1333.

[20] Huber W, von Heydebreck A, Sultmann H, Poustka A, and Vingron M (2002). Variance stabilization applied to microarray data calibration and to the quantification of differential expression. *Bioinformatics* **18**(suppl 1), S96–S104.

[21] Bühlmann P and Hothorn T (2007). Boosting algorithms: regularization, prediction and model fitting. *Stat Sci* **22**, 477–505.

[22] Hosmer DW and Lemeshow SA (1980). A goodness-of-fit test for the multiple logistic regression model. *Commun Stat* **A10**, 1043–1069.

[23] Harrell FE Jr, Lee KL, and Mark DB (1996). Multivariable prognostic models: issues in developing models, evaluating assumptions and adequacy, and measuring and reducing errors. *Stat Med* **15**, 361–387.

[24] Mekhail TM, Abou-Jawde RM, Boumerhi G, Malhi S, Wood L, Elson P, and Bukowski R (2005). Validation and extension of the Memorial Sloan-Kettering prognostic factors model for survival in patients with previously untreated metastatic renal cell carcinoma. *J Clin Oncol* **23**, 832–841.

[25] Sanchez-Navarro I, Gamez-Pozo A, Pinto A, Hardisson D, Madero R, Lopez R, San Jose B, Zamora P, Redondo A, Feliu J, et al. (2010). An 8-gene qRT-PCR-based gene expression score that has prognostic value in early breast cancer. *BMC Cancer* **10**, 336.

[26] Dweep H, Sticht C, Pandey P, and Gretz N (2011). miRWalk—database: prediction of possible miRNA binding sites by "walking" the genes of three genomes. *J Biomed Inform* **44**, 839–847.

[27] Thomas PD, Campbell MJ, Kejariwal A, Mi H, Karlak B, Daverman R, Diemer K, Muruganujan A, and Narechania A (2003). PANTHER: a library of protein families and subfamilies indexed by function. *Genome Res* **13**, 2129–2141.

[28] Thomas PD, Kejariwal A, Campbell MJ, Mi H, Diemer K, Guo N, Ladunga I, Ulitsky-Lazareva B, Muruganujan A, Rabkin S, et al. (2003). PANTHER: a browsable database of gene products organized by biological function, using curated protein family and subfamily classification. *Nucleic Acids Res* **31**, 334–341.

[29] Lu J, Getz G, Miska EA, Alvarez-Saavedra E, Lamb J, Peck D, Sweet-Cordero A, Ebert BL, Mak RH, Ferrando AA, et al. (2005). MicroRNA expression profiles classify human cancers. *Nature* **435**, 834–838.

[30] Edgar R, Domrachev M, and Lash AE (2002). Gene expression omnibus: NCBI gene expression and hybridization array data repository. *Nucleic Acids Res* **30**, 207–210.

[31] Motzer RJ, Bander NH, and Nanus DM (1996). Renal-cell carcinoma. *N Engl J Med* **335**, 865–875.

[32] Wang B, Howel P, Bruheim S, Ju J, Owen LB, Fodstad O, and Xi Y (2011). Systematic evaluation of three microRNA profiling platforms: microarray, beads array, and quantitative real-time PCR array. *PLoS One* **6**, e17167.

[33] Rini BI, Cohen DP, Lu DR, Chen I, Hariharan S, Gore ME, Figlin RA, Baum MS, and Motzer RJ (2011). Hypertension as a biomarker of efficacy in patients with metastatic renal cell carcinoma treated with sunitinib. *J Natl Cancer Inst* **103**, 763–773.

[34] Beuselinck B, Oudard S, Rixe O, Wolter P, Blesius A, Ayllon J, Elaidi R, Schoffski P, Barrascout E, Morel A, et al. (2011). Negative impact of bone metastasis on outcome in clear-cell renal cell carcinoma treated with sunitinib. *Ann Oncol* **22**, 794–800.

[35] Basappa NS, Elson P, Golshayan AR, Wood L, Garcia JA, Dreicer R, and Rini BI (2011). The impact of tumor burden characteristics in patients with metastatic renal cell carcinoma treated with sunitinib. *Cancer* **117**, 1183–1189.

[36] Terakawa T, Miyake H, Kusuda Y, and Fujisawa M (2011). Expression level of vascular endothelial growth factor receptor-2 in radical nephrectomy specimens as a prognostic predictor in patients with metastatic renal cell carcinoma treated with sunitinib. *Urol Oncol*. DOI:10.1016/j.urolonc.2011.1002.1012.

[37] Escudier B, Eisen T, Stadler WM, Szczylik C, Oudard S, Staehler M, Negrier S, Chevreau C, Desai AA, Rolland F, et al. (2009). Sorafenib for treatment of renal cell carcinoma: final efficacy and safety results of the phase III treatment approaches in renal cancer global evaluation trial. *J Clin Oncol* **27**, 3312–3318.

[38] Paule B, Bastien L, Deslandes E, Cussenot O, Podgorniak MP, Allory Y, Naimi B, Porcher R, de La Taille A, Menashi S, et al. (2010). Soluble isoforms of vascular endothelial growth factor are predictors of response to sunitinib in metastatic renal cell carcinomas. *PLoS One* **5**, e10715.

[39] Porta C, Paglino C, De Amici M, Quaglini S, Sacchi L, Imarisio I, and Canipari C (2010). Predictive value of baseline serum vascular endothelial growth factor and neutrophil gelatinase-associated lipocalin in advanced kidney cancer patients receiving sunitinib. *Kidney Int* **77**, 809–815.

[40] Farace F, Gross-Goupil M, Tournay E, Taylor M, Vimond N, Jacques N, Billiot F, Mauguen A, Hill C, and Escudier B (2011). Levels of circulating $CD45^{dim}CD34^{+}VEGFR2^{+}$ progenitor cells correlate with outcome in metastatic renal cell carcinoma patients treated with tyrosine kinase inhibitors. *Br J Cancer* **104**, 1144–1150.

[41] Gruenwald V, Beutel G, Schuch-Jantsch S, Reuter C, Ivanyi P, Ganser A, and Haubitz M (2011). Circulating endothelial cells are an early predictor in renal cell carcinoma for tumor response to sunitinib. *BMC Cancer* **10**, 695.

[42] Vermaat JS, van der Tweel I, Mehra N, Sleijfer S, Haanen JB, Roodhart JM, Engwegen JY, Korse CM, Langenberg MH, Kruit W, et al. (2010). Two-protein signature of novel serological markers apolipoprotein-A2 and serum amyloid alpha predicts prognosis in patients with metastatic renal cell cancer and improves the currently used prognostic survival models. *Ann Oncol* **21**, 1472–1481.

[43] van der Veldt AA, Eechoute K, Gelderblom H, Gietema J, Guchelaar HJ, van Erp NP, van den Eertwegh AJ, Haanen JB, Mathijssen RH, and Wessels JA (2011). Genetic polymorphisms associated with a prolonged progression-free survival in patients with metastatic renal cell cancer treated with sunitinib. *Clin Cancer Res* **17**, 620–629.

[44] Weng L, Wu X, Gao H, Mu B, Li X, Wang JH, Guo C, Jin JM, Chen Z, Covarrubias M, et al. (2010). MicroRNA profiling of clear cell renal cell carcinoma by whole-genome small RNA deep sequencing of paired frozen and formalin-fixed, paraffin-embedded tissue specimens. *J Pathol* **222**, 41–51.

[45] Petillo D, Kort EJ, Anema J, Furge KA, Yang XJ, and Teh BT (2009). MicroRNA profiling of human kidney cancer subtypes. *Int J Oncol* **35**, 109–114.

[46] Youssef YM, White NM, Grigull J, Krizova A, Samy C, Mejia-Guerrero S, Evans A, and Yousef GM (2011). Accurate molecular classification of kidney cancer subtypes using microRNA signature. *Eur Urol* **59**, 721–730.

[47] Lin J, Horikawa Y, Tamboli P, Clague J, Wood CG, and Wu X (2010). Genetic variations in microRNA-related genes are associated with survival and recurrence in patients with renal cell carcinoma. *Carcinogenesis* **31**, 1805–1812.

[48] Slaby O, Jancovicova J, Lakomy R, Svoboda M, Poprach A, Fabian P, Kren L, Michalek J, and Vyzula R (2010). Expression of miRNA-106b in conventional renal cell carcinoma is a potential marker for prediction of early metastasis after nephrectomy. *J Exp Clin Cancer Res* **29**, 90.

[49] Olson P, Lu J, Zhang H, Shai A, Chun MG, Wang Y, Libutti SK, Nakakura EK, Golub TR, and Hanahan D (2009). MicroRNA dynamics in the stages of tumorigenesis correlate with hallmark capabilities of cancer. *Genes Dev* **23**, 2152–2165.

[50] Burczynski ME, Twine NC, Dukart G, Marshall B, Hidalgo M, Stadler WM, Logan T, Dutcher J, Hudes G, Trepicchio WL, et al. (2005). Transcriptional profiles in peripheral blood mononuclear cells prognostic of clinical outcomes in patients with advanced renal cell carcinoma. *Clin Cancer Res* **11**, 1181–1189.

[51] Twine NC, Stover JA, Marshall B, Dukart G, Hidalgo M, Stadler W, Logan T, Dutcher J, Hudes G, Dorner AJ, et al. (2003). Disease-associated expression profiles in peripheral blood mononuclear cells from patients with advanced renal cell carcinoma. *Cancer Res* **63**, 6069–6075.

[52] Wulfken LM, Moritz R, Ohlmann C, Holdenrieder S, Jung V, Becker F, Herrmann E, Walgenbach-Brunagel G, von Ruecker A, Muller SC, et al. (2011). MicroRNAs in renal cell carcinoma: diagnostic implications of serum miR-1233 levels. *PLoS One* **6**, e25787.

[53] Heng DY, Chi KN, Murray N, Jin T, Garcia JA, Bukowski RM, Rini BI, and Kollmannsberger C (2009). A population-based study evaluating the impact of sunitinib on overall survival in the treatment of patients with metastatic renal cell cancer. *Cancer* **115**, 776–783.

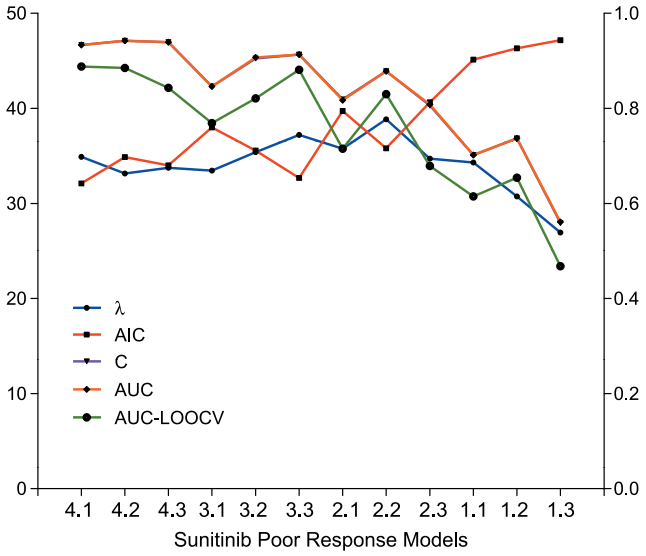

Figure W1. Discriminant power of poor response predictive signatures. *λ*, correlation shrinkage intensity; AIC, Akaike information criterion; *c*, Harrell's bias-corrected concordance index; AUC, area under the ROC curve; AUC-LOOCV: leave-one-out cross-validated area under the ROC curve. All variables are referred to the right *y*-axis except for AIC. AUC and *c* partially overlap.

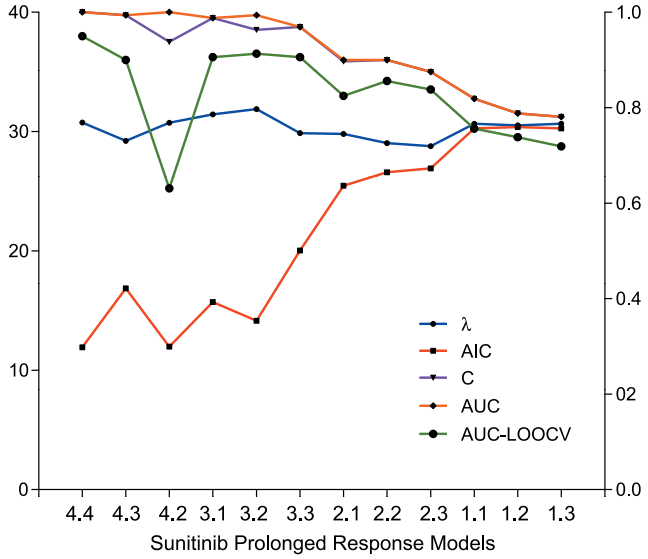

Figure W2. Discriminant power of prolonged response predictive signatures. All variables are referred to the right *y*-axis except for AIC. AUC and *c* partially overlap.

Table W1. PD-Free Survival in Poor and Prolonged Response Models.

Model	%PDFS 6 m PoorR	%PDFS 6 m Response	HR	95% CI
PoorR 4.1	20	85.7	5.64	1.925–16.54
PoorR 4.2	16.6	92.3	2.87	1.14–7.22
PoorR 4.3	10	89.3	18.54	5.21–66.01
PoorR 3.1	30	82.14	1.89	0.75–4.71
PoorR 3.2	33.33	79.31	1.81	0.69–4.73
PoorR 3.3	27.27	85.18	2.76	1.11–6.87
PoorR 2.1	25	80	3.74	1.24–11.35
PoorR 2.2	41.67	80.77	1.65	0.72–3.75
PoorR 2.3	16.67	78.12	8.23	1.92–35.13

Model	%PDFS 18 m ModR	%PDFS 18 m ProR	HR	95% CI
ProR 4.1	0	100	16.4	5.34–50.38
ProR 4.2	6.67	90	10.47	3.63–30.13
ProR 4.3	0	100	16.4	5.34–50.38
ProR 3.1	6.67	90	4.66	1.74–12.48
ProR 3.2	6.67	90	11.73	3.98–34.51
ProR 3.3	13.33	80	9.12	3.09–26.93
ProR 2.1	18.75	77.78	3.42	1.33–8.75
ProR 2.2	13.33	80	5.05	1.90–13.41
ProR 2.3	23.53	75	2.72	1.05–7.03

PDFS, PD-free survival; m, months; PoorR, poor response; ProR, prolonged response; ModR, moderate response; HR, hazard ratio; 95% CI, 95% confidence interval.

Table W2. miRWalk-Validated Genes Targeted by Poor Response and Prolonged Response miRNAs.

miRNA	Response Model	Gene
hsa-miR-125a-5p	Poor	*CD2*, *CTNNB1*, *NBN*, *FMR1*, *DICER1*, *IGF2BP2*, *COX8A*, *PRDM1*, *TNFSF11*, *CD4*, *ELA2*, *ATM*, *MOV10*, *CCL5*, *CTGF*, *CDKN1A*, *BCL2*, *G3BP2*, *RRBP1*, *GPI*, *PCNA*, *TNRC6B*, *KLF13*, *ETS2*, *PDPN*, *CTSD*, *ODZ1*, *BRCA1*, *TCF7L2*, *POLR2K*, *CDKN2D*, *LCT*, *RAB30*, *EGFR*, *ERBB2*, *HSPG2*, *IGF1R*, *LIF*, *TLE1*, *RB1*, *LIN28*, *MDM2*, *JUNB*, *ETV4*, *ERBB3*, *IGFBP5*, *FZD7*, *TP53*, *MAP2K7*, *MECP2*, *ELAVL1*, *IL10*, *IGFBP6*, *RNASEN*, *SLC9A3R1*, *BAP1*, *UBE2N*, *PCDH8*, *MAPK3*, *INS*, *RHOU*, *PCAF*, *USP7*, *PDGFRB*, *TLR4*, *KPNA2*, *MYC*, *SOX17*, *MED6*, *RCHY1*, *PSMD2*, *APC*, *NR1I2*, *MRE11A*, *NTRK3*, *WNT10A*, *BCL2L11*, *CD40LG*, *MTUS1*, *AHSA1*, *ATF1*, *PEA15*, *PSMA7*, *RNASEH2A*, *BRCA2*, *IFNA1*, *RARA*
hsa-miR-139-3p	Poor	*SSSCA1*, *CDC73*, *ROCK2*, *RHOD*, *CDKN1B*
hsa-miR-141	Poor	*ACTG1*, *AHSA1*, *AKT1*, *AKT1*, *AMACR*, *ARS2*, *BMP2*, *BRD3*, *C6orf134*, *CCND1*, *CCND2*, *CCNT2*, *CD79A*, *CDC25C*, *CDH1*, *CDH17*, *CDKN1B*, *CDON*, *CREB1*, *CSH1*, *CSNK1A1*, *DHH*, *DLC1*, *DMTF1*, *EGF*, *EIF4E*, *ERBB4*, *ETS1*, *EZH2*, *FBXW11*, *FBXW7*, *FOXA2*, *FOXC2*, *FOXE1*, *FOXF1*, *FOXL1*, *FOXP3*, *FZR1*, *GLI1*, *GLI2*, *GLI3*, *GPD1*, *HIF1A*, *HOXD10*, *HPRT1*, *IHH*, *INHBC*, *INHBE*, *JAG2*, *JUN*, *JUN*, *KCNMA1*, *KIAA0152*, *KLF5*, *KLF8*, *KLK3*, *LAMC2*, *LARP6*, *LOX*, *MAP2K4*, *MAP3K10*, *MAPK14*, *MAPK9*, *MAPKAPK5*, *MET*, *MYB*, *MYC*, *MYCN*, *NPC1*, *PARP8*, *PDCD4*, *PIK3CA*, *PLCG1*, *PLEKHM1*, *PLUNC*, *POU3F1*, *PPIA*, *PSAT1*, *PTEN*, *PTPN12*, *PTPN13*, *PTPN14*, *RAPGEF5*, *RHOD*, *RIT2*, *RPIA*, *RUNX2*, *SEMA6A*, *SFRP1*, *SFRP1*, *SFRS2IP*, *SHH*, *SIDT1*, *SIP1*, *SLC12A1*, *SLC9A3R2*, *SMC1A*, *SNAI1*, *SNAI2*, *SNAI3*, *SOX13*, *SSSCA1*, *STK24*, *STK3*, *SUFU*, *SULT2A1*, *TACSTD1*, *TBP*, *TBX2*, *TCF21*, *TGFB1*, *TGFB2*, *TMEM184B*, *TMOD3*, *TP53*, *TPPP3*, *TWIST1*, *TWIST2*, *UBAP1*, *VEGFA*, *VEGFA*, *YAP1*, *ZEB1*, *ZEB2*, *ZFPM2*, *ZNF135*, *ZNF77*
hsa-miR-145	Poor	*RNASEN*, *STAT1*, *PDGFB*, *RNASEN*, *EIF4EBP1*, *SRGAP2*, *MMP9*, *KLF4*, *RBBP6*, *SOX2*, *PAK3*, *CDK4*, *IGF1*, *DGCR8*, *ADAM17*, *BCL2*, *MYC*, *MCL1*, *ERBB2*, *MYH11*, *KCNH8*, *TP53*, *EWSR1*, *BNIP3*, *EIF4E*, *IGF1R*, *SOD2*, *YES1*, *CBFB*, *PAK1*, *CCND1*, *COX8A*, *SMTN*, *NKX2-3*, *TP73*, *FLI1*, *MUC1*, *IRS1*, *WT1*, *VANGL1*, *PPP3CA*, *PTEN*, *CCNG1*, *ODZ1*, *TAGLN*, *KLF5*, *CKAP4*, *MYO6*, *FABP4*, *ASAHL*, *DICER1*, *AKT1*, *CLINT1*, *ZEB1*, *KRAS*, *EGFR*, *SRC*, *PGK1*, *KRT7*, *CD2AP*, *SFRS8*, *SRF*, *RREB1*, *PPP2R1B*, *GALNT1*, *EGF*, *RTKN*, *PPIA*, *HOXA9*, *CAP1*, *EPHB2*, *DDX5*, *EIF2C1*, *FSCN1*, *SOX4*, *FRAP1*, *SWAP70*, *ACTA2*, *EIF2C2*, *IFNA1*, *ESR1*, *CDH11*, *FCER2*, *RPS14*, *CDKN1A*, *POLD3*, *DFFA*, *RPS6KB1*, *CTNNB1*, *TGFBR2*, *CLEC4G*, *BIRC2*, *ERCC8*, *DFFB*, *SMPD1*, *F11R*, *SOX18*, *E2F3*, *ROBO2*, *MMP3*, *NKX2-5*, *TNFSF10*, *TSC2*, *BEX1*
hsa-miR-150	Poor	*IL6*, *ZAP70*, *SSSCA1*, *MYB*, *CCND1*, *NFKB1*, *SLC35B2*, *CD4*, *PRKCA*, *RELB*, *CDK4*, *FOXP1*, *CD8A*, *BCR*, , *CLCN3*, *P2RX7*, *USF2*, *CAPNS1*, *MAP3K8*, *BCL2*, *MCL1*, *EGR2*, *PTGS1*, *IRAK2*, *TNFSF10*, *AGTR1*, *IL17A*, *CTSL1*, *RAC1*, *IRAK4*, *FGF7*, *RAB27A*, *ALG2*, *ZIC3*, *FASN*, *KIT*, *JAK2*, *IKBKE*, *IGF1*, *CNTN3*, *TSHZ3*
hsa-miR-181a*	Poor	*NPM1*, *PML*, *PDK4*, *PSMD9*, *MMP9*, *SSSCA1*, *CDX2*, *WT1*, *DMPK*, *DICER1*, *TGFB1*, *CD36*, *GPI*, *BAALC*, *NBN*, *RNASEN*, *TIMP3*, *GYPA*, *TACSTD1*, *ZFPM1*, *LCT*, *DGCR8*, *TFRC*, *BCL2*, *GATA6*, *FLT3*, *NTS*, *RDX*, *NLK*, *MECP2*, *NPM1*, *ODZ1*, *ELA2*, *IL6*, *CEBPA*, *ATM*, *PTEN*, *HOXA11*, *MT4*, *SUFU*, *EPOR*, *BCL2L11*, *THRB*, *STAT1*, *CD4*, *TWIST1*, *ERG*, *BCR*, *RC3H1*, *CDKN1B*, *CD8A*, *SOCS1*, *LYN*, *TSPO*, *RASSF1*, *GATA1*, *MCL1*, *ALAS1*, *DCTN6*, *SMAD4*, *ERBB2*, *AFP*
hsa-miR-192	Poor	*DICER1*, *SLC9A3R2*, *RAPGEF5*, *NODAL*, *FOXA1*, *DNAI1*, *CDKN1A*, *SSSCA1*, *CTNNB1*, *RAG2*, *COL1A2*, *ZEB2*, *AKT1*, *FGF3*, *CCND2*, *PAK3*, *SMAD2*, *BRAF*, *COL4A1*, *TGFB1*, *PTEN*, *BRCA1*, *ALCAM*, *CYCS*, *SMAD3*, *APC*, *TP53*, *ZEB1*, *CDH1*, *DICER1*, *CCND1*, *CYP7A1*, *BIRC5*, *SMAD7*, *TYMS*, *TFE3*, *IFNG*, *COL1A1*, *APOE*, *AMACR*, *USF1*, *PIK3CA*, *IL1B*, *CTGF*, *SLC22A3*, *MDM2*, *MSH2*, *NOS2A*, *SIP1*, *ITK*, *CD79A*, *MLH1*, *TNF*, *BBS9*, *FADD*, *KRAS*, *MLC1*, *BMP6*, *RAD9A*, *MCL1*, *MSH6*, *SFRS2IP*, *HNF1A*, *NUMA1*, *HNF4A*, *TNPO1*, *EGFR*
hsa-miR-193a-3p	Poor	*MCL1*, *NOS2A*, *PTK2*, *TNF*, *BRAF*, *CTNNB1*, *NRAS*, *DNMT1*, *CD4*, *TP53*, *CD8A*, *TP73*, *CD28*, *CKAP4*, *E2F3*, *CYP7A1*, *CDK6*, *IFNG*
hsa-miR-193a-5p	Poor and prolonged	*NRAS*, *CD4*, *CD8A*, *CD28*, *CTNNB1*, *CDK6*, *DNMT1*, *NCOA2*, *TP53*, *MCL1*, *TP73*, *PTK2*, *CKAP4*, *TGFB1*, *BRAF*
hsa-miR-199a-5p	Poor and Prolonged	*PI3*, *AMELX*, *FASLG*, *AKT1*, *MAPK14*, *NEUROD1*, *CALB1*, *FASN*, *CD44*, *ALOX5*, *EZH2*, *PTEN*, *IKBKB*, *MAPK8*, *ALOX5AP*, *PRNP*, *SIRT1*, *MAPK9*, *ENAM*, *DDR1*, *TWIST1*, *RNMT*, *COX8A*, *HIF1A*, *DECR1*, *SOX9*, *INSR*, *CYP2A6*, *NFKB1*, *EGFL7*, *PPIG*, *CRYGC*, *MET*, *PRKG1*, *MAPK1*, *AHSA1*
hsa-miR-30b*	Poor	*ARHGDIA*, *GPR172B*, *STRN*, *NAPG*, *REG3A*, *KLK8*, *GAK*, *SLC38A5*, *GSTM4*, *HSD17B12*, *PTPRK*, *SHOC2*, *TGFBR1*, *WDR68*, *EIF4E*, *HBXIP*, *VPS39*, *MLLT1*, *TRMU*, *WNT5A*, *YIF1B*, *LHX1*, *DNAJC19*, *ARFIP1*, *FHL5*, *HSPA1A*, *PGM1*, *BCKDHB*, *ABHD11*, *ARID4B*, *JUN*, *FAM105A*, *GNPNAT1*, *LMNB2*, *SLC12A2*, *PRSS21*, *SLC7A11*, *NOTCH2*, *SCYL1*, *DHX40*, *RUNX2*, *SHH*, *ADSS*, *FADS1*, *PPP1R7*, *SYPL1*, *TNFRSF10B*, *DMN*, *PRAF2*, *TXN2*, *GPR56*, *SAC3D1*, *NT5C3*, *PURA*, *AARSD1*, *CHST14*, *CALCOCO2*, *PTPLB*, *RPP38*, *SYNE1*, *MOV10*, *BRWD2*, *CA12*, *IGF1*, *ASH2L*, *DICER1*, *GRPEL2*, *CHMP2A*, *SLC4A7*, *HSPA1B*, *SERPINE2*, *RCN2*, *HSDL1*, *TAC1*, *AGRN*, *TMCO1*, *CDCP1*, *DOCK7*, *TOMM34*, *TMEM2*, *NP*, *PTGS2*, *IPO4*, *GARS*, *CYP51A1*, *FADS3*, *PPP2R4*, *THBS1*, *TNFRSF10A*, *DMD*, *DUSP12*, *METTL7A*, *MARS2*, *SNX15*, *PDE3A*, *PTBP2*, *SLC25A32*, *HIPK3*, *AKAP8*, *F2*, *UTRN*, *SPTLC1*, *KIAA0776*, *TMEM41B*, *CEP72*, *SLC30A1*, *CCND1*, *CLDN1*, *DGCR8*, *CPOX*, *RAB30*, *FXR2*, *DNAJB1*, *ATP6V1C1*, *RHEB*, *ATAD3B*, *KCNN4*, *GNL3L*, *MRPS24*, *AP3B1*, *UBE2I*, *TMED2*, *SH3BP4*, *ATP2A2*, *NUFIP2*, *SLC25A22*, *SMAD3*, *RNASEN*, *AP2A1*, *ARL2*, *PPP2R5C*, *TLOC1*, *PEX11B*, *ID1*, *LYPLA2*, *GALNT1*, *ATP6V1F*, *DPP7*, *UBE2J1*, *SRPRB*, *SLC38A1*, *CDKN2A*, *OPRS1*, *ARL5B*, *RAB34*, *VSNL1*, *PDLIM5*, *KIAA0409*, *MTRR*, *CAND1*, *LUZP1*, *CLTC*, *DHX57*, *GRIA2*, *PTRH1*, *GNAI2*, *SCAMP1*, *HYAL1*, *ACP2*, *SPCS3*, *KPNA3*, *ATRX*, *SLC1A4*, *GFM1*, *GAPDH*, *MLLT11*, *PISD*, *NPR3*, *AADACL1*, *GEMIN7*, *ESR1*, *NKX2-3*, *ZNF384*, *LPL*, *PPP3CA*, *TNFAIP2*, *NRP1*, *ITGB3*, *FMNL2*, *TMEM87A*, *TRIP13*, *SLC25A24*, *ANKFY1*, *SNX6*, *COIL*, *FSTL1*, *BET1*, *FGF2*, *UTP15*, *ACVR1B*, *IGF2BP1*, *TMED3*, *MYO1E*, *PRKCI*, *CACNA2D1*, *IFNA1*, *SLC16A3*, *EIF2C2*, *KDELC2*, *GPD2*, *MPDU1*, *IDH1*, *PLK1*, *CCL13*, *TMEM189*, *LY6K*, *SLC7A1*, *SSNA1*, *IRAK2*, *TMED10*, *IFIT5*, *NT5E*, *WDFY1*, *EHMT1*, *TGFB1*, *TPPP*, *DSG2*, *LRP1*, *PPP3R1*, *TPM1*, *SQSTM1*, *PTPMT1*, *ZNF294*, *VAMP3*, *PSAT1*, *PTPLAD1*, *RAB6A*, *UNC93B1*, *MAPK14*, *CDIPT*, *FGF13*, *SDCBP*, *STX7*, *KIAA0152*, *GNA13*, *HARS2*, *MYO10*, *PKN2*, *PXDN*, *BCL6*, *RQCD1*, *CPNE8*, *TTC9C*, *TMEM59*, *IFRD1*, *ATP6V0A1*, *RHOB*, *PPIB*, *MAP2K1IP1*, *JAK2*, *FERMT2*, *NAT6*, *NUCB1*, *RNF213*, *AGMAT*, *CHAF1A*, *DSP*, *TACSTD2*, *ABHD10*, *TPM2*, *AP3D1*, *AKT1*, *THEM4*, *RAI14*, *SNAP29*, *GYS1*, *TAF9B*, *RAB27B*, *CAPG*, *C1D*, *FNDC3A*, *POLE3*, *NCAPG*, *MLSTD2*, *TNFSF11*, *CTSC*, *TRAM1*, *HNRPM*, *LRRC8A*, *IFRD2*, *PRDM1*, *RFT1*, *OAS1*, *CSNK1D*, *SFI1*, *AMIGO2*, *KRT85*, *CDKAL1*, *SLC12A4*, *CBFB*, *HMGA2*, *CHD1*, *PANX1*, *SPRYD4*, *PAFAH1B2*, *GPAM*, *MRM1*, *ZIC1*, *ABCF2*, *DSPP*, *SMAD1*, *PPP5C*, *TPM3*, *P4HA2*, *XIAP*, *GALNTL2*, *SLC9A3R2*, *ANXA2*, *MRPS33*, *RAB5C*, *ARID1A*, *GJA1*, *SEC23A*, *TRIM32*, *PODXL*, *NXN*, *FAM96A*, *PAH*, *MTHFD2*, *CARHSP1*, *NARS*, *POLE4*, *ATG9A*, *SOX2*, *AURKB*, *NOTCH1*, *CSRP1*, *MRC2*, *IGF2R*, *RHOG*, *PPL*, *SLC25A1*, *RNMT*, *SLC6A3*, *DNAJB4*, *FRG1*, *ARL10*, *TMED7*, *KIAA1618*, *DOCK5*, *SMAD2*, *PPIF*, *PHC2*, *MAT2A*, *PRIM1*, *TXNRD1*, *PHLDB2*, *BCL2*, *CLN5*, *GFPT1*, *UBE4A*, *HARS*, *CDK5RAP1*, *RAD23B*, *PICALM*, *VTI1B*, *PLXND1*, *TICAM2*, *POLD2*, *ATG3*, *LRRC8C*, *SEC24A*, *CORO1C*, *NCL*, *RTN4*, *TMEM109*, *LIN28*, *PAX3*, *CTNNB1*, *RBM19*, *LAMC1*, *DUSP23*, *UAP1*, *TNFSF9*, *SNCA*, *PWP1*, *LYCAT*, *PDLIM7*, *ANPEP*, *TXNDC12*, *PTPRF*, *NARG1*, *MET*, *SLC25A13*, *EGFR*, *MBNL1*, *TRMT1*, *TYMS*, *MPZL1*, *TP53*, *MSI2*, *CHORDC1*, *SFXN1*, *HMGA1*, *RAB23*, *RARS*, *ADPGK*, *MYLIP*, *CEBPB*, *RCOR1*, *ITGA2*, *POLR2C*, *MOSC1*, *CUL4B*, *RELA*, *PGRMC1*, *ARFIP2*, *NEDD4*, *PTBP1*, *BAT2*, *ALPL*, *PAX6*, *RDH10*, *LCP1*, *MRPL20*, *SRPR*, *SNAP23*, *NOS1*, *SEC23IP*, *ELMOD2*, *DTD1*, *COMMD9*, *GOLGA7*, *PTPRJ*, *CDK5RAP3*, *RCAN2*, *ARID2*, *SYNE2*, *PRPF40A*, *UGT8*, *ZNF622*, *DNM1L*, *IQGAP3*, *BRPF3*, *FADS2*, *HMOX1*, *GALNT7*, *RBMS1*, *SH3BGRL3*, *ANP32B*, *ITGB4*, *SLC38A2*, *FNDC3B*, *GTPBP3*, *BDNF*, *EHMT2*, *POLA2*, *NELL1*, *PTGFRN*, *TMEM43*, *BMP2*, *TRIM27*, *MOSPD2*
hsa-miR-31	Poor and Prolonged	*BAMBI*, *FOXP3*, *TP53*, *MCM2*, *HBEGF*, *DACT3*, *SP7*, *CCL16*, *ODZ1*, *HRSP12*, *TIAL1*, *JAK2*, *TBX1*, *MID1*, *PPP6C*, *PTEN*, *CASR*, *TIMP2*, *MYB*, *SATB2*, *BGLAP*, *CD4*, *FGFR3*, *HIF1A*, *VSNL1*, *PRB1*, *BIN3*, *RUNX2*, *ETS1*, *PRKD1*, *HMGA2*, *HIF1AN*, *CCT4*, *RHOA*, *CDKN2B*, *FOS*, *WASF3*, *ICAM1*, *CDKN2A*, *ITGA5*, *MTAP*, *PPP2R2A*, *KRT15*, *DCN*, *SELE*, *CDKN2D*, *RDX*, *PGGT1B*, *PPP2R4*, *PDLIM7*, *SFRP1*, *TNF*, *BCL2L2*, *DLX3*, *TRIM36*, *LATS2*, *JAG1*, *COX8A*, *SFRP4*, *TIAM1*, *KRT16*, *BAX*, *STMN1*, *WIF1*, *E2F3*, *KRT17*, *E2F2*, *ERCC4*, *MYC*, *DKK1*, *IBSP*

Table W2. (*continued*)

miRNA	Response Model	Gene
hsa-miR-34a	Poor and Prolonged	*CD47*, *TP53*, *CDK4*, *RUNX2*, *LOX*, *CNN3*, *E2F3*, *G6PD*, *VEGFA*, *MDM2*, *BCL2*, *LEF1*, *MDC1*, *CAV1*, *E2F1*, *EPHB2*, *TBK1*, *HELLS*, *CDK6*, *AKT1*, *IRS1*, *MYC*, *PPARG*, *PTPN13*, *EIF2C4*, *MITF*, *FASN*, *DLL1*, *HDAC9*, *RB1*, *BCL6*, *CDKN1A*, *SIRT1*, *STK39*, *RNMT*, *MAP2K1*, *MYBL1*, *SLC11A1*, *CCND1*, *BIRC3*, *TOM1*, *TLR4*, *MAP1LC3A*, *COL11A2*, *GRM7*, *CREB1*, *BAMBI*, *SFRP1*, *ELK3*, *HES1*, *HOXA5*, *PIK3CA*, *HNF4A*, *LIF*, *CCNE2*, *ACSL1*, *APC*, *CREBZF*, *CCND3*, *MET*, *MAP3K9*, *NDRG1*, *PTEN*, *CRIM1*, *SLC12A1*, *ATP6V1B2*, *MYCN*, *MECP2*, *ZEB1*, *NOTCH1*, *OCA2*, *ZAP70*, *SMARCA5*, *JAG1*, *CDC25C*, *BCR*, *BNIP3L*, *CDC25A*, *RGS3*, *CD44*, *COL2A1*, *E2F5*, *CDKN2A*, *TCF21*, *IFNG*, *POU4F2*, *FRAP1*, *ZEB2*, *ACTB*, *SLC2A1*, *ANP32B*, *JARID1B*, *NDUFA2*, *PPP1R13L*, *SND1*, *BRAP*, *ING2*, *NR1H4*, *IL1B*, *GABPA*, *FOXP1*, *COX8A*, *DICER1*, *SSSCA1*, *PEA15*, *BBC3*, *WNT1*, *MYB*, *RTEL1*, *SCPEP1*, *TIMM8A*, *FOXO1*, *LIN28*, *PTPN12*, *MAPK14*, *NOS2A*, *BDNF*, *MGST1*, *MDM4*, *KRAS*, *SEMA6A*, *DDIT4*, *ST3GAL4*, *PROM1*, *ECD*, *ARCN1*, *CXCL12*, *NFE2L2*, *ATN1*, *HMG2L1*, *HMGA2*, *YY1*, *SEC24D*, *MAPKAPK2*, *HDAC2*, *GRM3*, *VAMP2*, *TCL1A*, *TNRC6A*, *ARIH2*, *CTNNBIP1*, *NFKB1*, *BAX*, *ZNF135*, *ERBB4*, *DDX4*, *CSF1*, *PHGDH*, *UBL4A*, *SPI1*, *CISH*, *SFRS2*, *FOXJ1*, *PAWR*, *AXIN2*, *NOL3*, *CDC20B*, *ZNF77*, *KCNMA1*, *LARP4*, *PRMT5*, *EZH2*, *KLF4*, *RPS19*, *CEBPA*, *DKK2*, *RNASEN*, *NPC1*
hsa-miR-370	Poor	*TCF4*, *ZEB2*, *WBSCR22*, *ZEB1*, *BRD8*, *TGFB1*, *ACACA*, *TGFB2*, *CPT1A*, *FASN*, *SREBF1*, *SPARC*, *DGAT2*, *TCF4*, *KIT*, *HMGA2*, *PDGFRA*, *TAGLN2*, *HMGA1*, *MAP3K8*, *IL6*
hsa-miR-505*	Poor	*ARSF*, *CDKN2A*, *CDKN2D*, *ELF4*, *SFRS1*, *TP53*, *C5orf41*
hsa-miR-516a-5p	Poor	*KLK10*
hsa-miR-564	Poor and Prolonged	*DICER1*
hsa-miR-582-5p	Poor	*TGFB1*, *DLK1*, *SMAD3*, *SMAD6*, *SMAD9*
hsa-miR-659	Poor and Prolonged	*GRN*
hsa-miR-126*	Prolonged	*TLR4*, *ACVR2A*, *UBASH3A*, *EGF*, *SOX2*, *EGFL7*, *POLR2A*, *CEBPZ*, *CRK*, *PIK3R2*, *SRY*, *PIK3CA*, *CREB1*, *VEGFA*, *SPRED1*, *JUN*, *PECAM1*, *TOM1*, *DICER1*, *PLK2*, *SRC*, *KDR*, *SLC45A3*, *PLAC1*, *AKT1*, *CASP3*, *GLI1*, *RNASEN*, *WT1*, *EGFR*, *HOXA9*, *CD4*, *SOX4*, *EPHB2*, *CXCL12*, *KRAS*, *MYB*, *HNF1A*, *CD8A*, *MERTK*, *CD70*, *PI3*, *CXCR4*, *NRAS*, *CD2AP*, *FOXJ2*, *TGFBR2*, *RHOC*, *CD28*, *PTPRN2*, *DNMT1*, *MRGPRX3*, *SMOX*, *MAPK8*, *ETS1*, *CD44*, *ITGA2B*, *ITGAL*, *COX8A*, *PTEN*, *C9orf127*, *ETS2*, *HOXD10*, *MAFB*, *FLI1*, *SMO*, *HPS1*, *TNC*, *HOXA1*, *CDKN1A*, *PDGFB*, *TP53*, *IL1B*, *RUNX1*, *PAK1*, *GATA3*, *TP63*, *CCND1*, *VCAM1*, *TLR2*, *JAK2*, *RUNX1T1*
hsa-miR-1274a	Prolonged	*CYP7A1*, *IFNG*, *IL1B*, *NOS2A*, *TNF*, *AASDHPPT*
hsa-miR-136	Prolonged	*ME1*, *RRBP1*
hsa-miR-198	Prolonged	*ESR1*, *BRCA1*, *GJA1*, *TUSC2*, *GRIA2*, *FUS*, *MYLIP*, *CCND1*, *NOTCH1*, *CCND2*, *ARID4B*, *ATF2*, *TAC1*, *JUN*, *HIPK3*, *UTRN*, *PTPN1*, *CDKN2A*, *VSNL1*, *TAF1*, *FSTL1*, *ACVR1B*, *MAPK14*, *KIAA0152*
hsa-miR-199a-3p	Prolonged	*AKT1*, *BMP2*, *COMP*, *EPHB2*, *FRAP1*, *GARS*, *MET*, *PIK3CA*, *PTEN*, *RAG2*, *RB1*, *SOX9*, *TIMM8A*, *TNF*
hsa-miR-371-5p	Prolonged	*DNMT3A*, *DNMT3B*, *FABP4*, *ADIPOQ*, *TP53*, *LATS2*
hsa-miR-376a	Prolonged	*PRPS1*, *SLC16A1*, *TTK*, *SFRS11*, *RHOD*, *ZNF513*, *PRPS1L1*, *SNX19*
hsa-miR-410	Prolonged	*JUN*, *NFKB1*, *RB1*, *TP53*, *PUM1*, *COX8A*, *MAPK1IP1L*, *CDC2*, *CDKN2A*
hsa-miR-424*	Prolonged	*CCND3*, *GTF2IRD1*, *CEBPB*, *NIT1*, *CDKN1A*, *CCNE1*, *SETD2*, *EGFR*, *MED1*, *CREB1*, *MAPK9*, *CHEK1*, *CCNF*, *BCR*, *MUC1*, *OPRS1*, *ATF2*, *MAP2K1*, *ETS1*, *CCNE2*, *FLT3*, *LGALS3*, *CHD4*, *E2F3*, *RASA1*, *ATF6*, *KIF23*, *SPINK1*, *DDX20*, *AP2M1*, *HOXA4*, *CCND1*, *TAF10*, *EIF2C1*, *CDC25A*, *E2F1*, *EIF2C2*, *DDX5*, *NFE2L1*, *ARPC5L*, *PAK3*, *PLAG1*, *ESR1*, *FGFR1*, *NFE2L2*, *MYB*, *ANLN*, *SMAD3*, *PIAS1*, *NCOA6*, *SP3*, *SIAH1*, *POU2F2*, *SYNGAP1*, *FOSB*, *USF2*, *BCL6*, *LATS2*, *CDK6*, *RARA*, *MBD4*, *INPPL1*, *YY1*, *WEE1*, *CUL2*, *RNASEN*, *RXRA*, *RUNX1*, *ITPR1*, *KCNH8*, *CDC14A*, *HIF1A*
hsa-miR-630	Prolonged	*H2AFX*, *CDKN1A*, *TP53*, *CISH*, *SSSCA1*, *GADD45A*, *TP73*, *YES1*, *YAP1*, *PARP1*, *HIPK2*, *ATM*, *BCL2*, *BAX*, *BCL2L2*, *CDKN1B*, *CASP3*

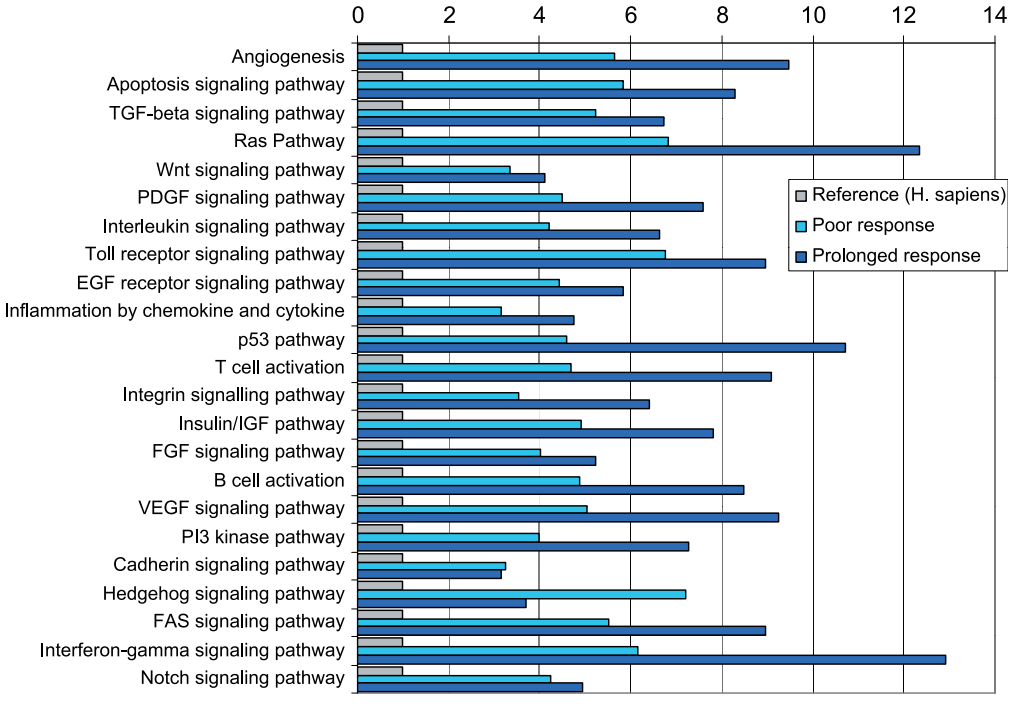

Figure W3. Pathways overrepresented by action of poor response and prolonged response miRNAs.

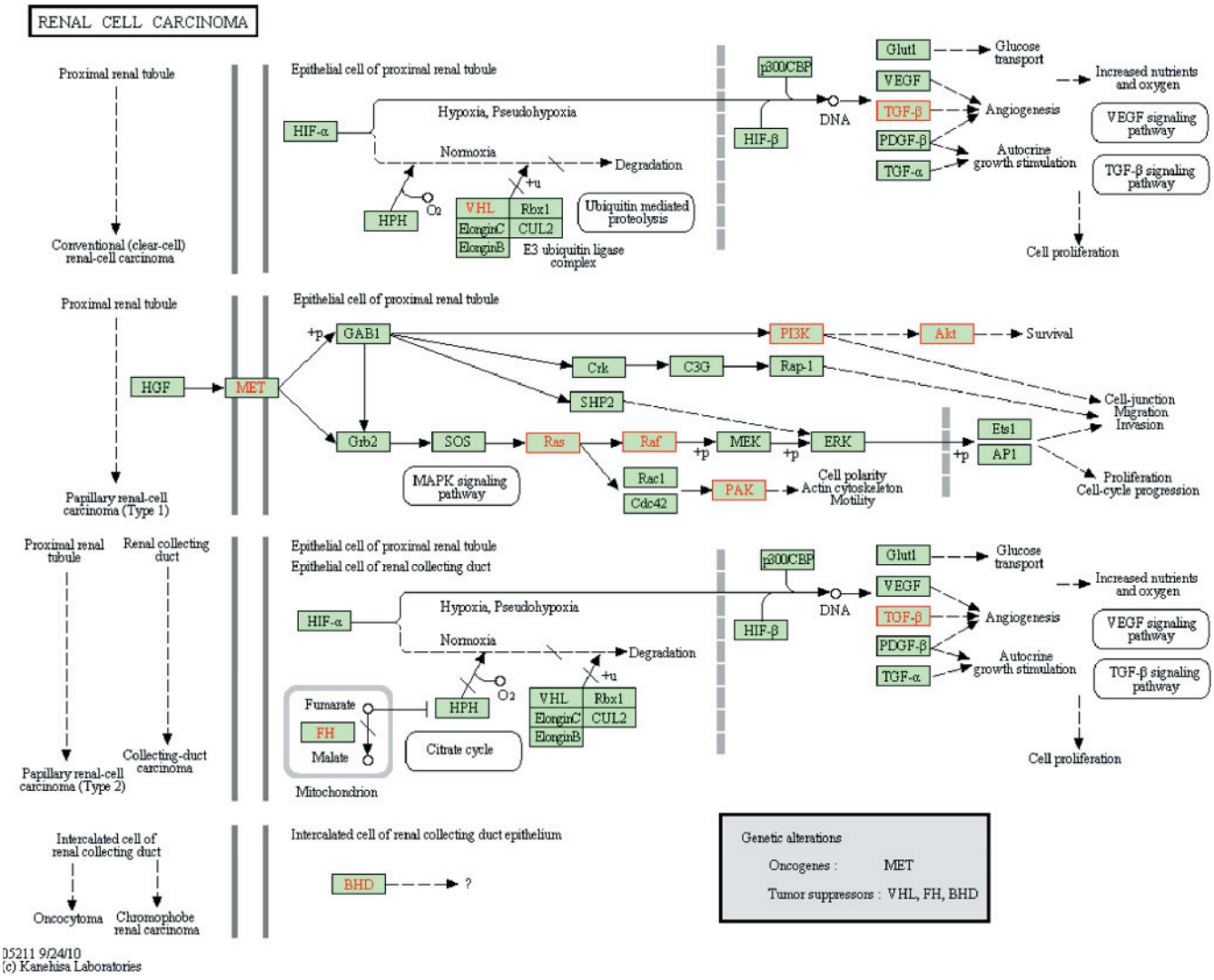

Figure W4. RCC pathway and poor response genes. Genes from KEGG RCC pathway targeted by miRNAs (red) included in poor response models.

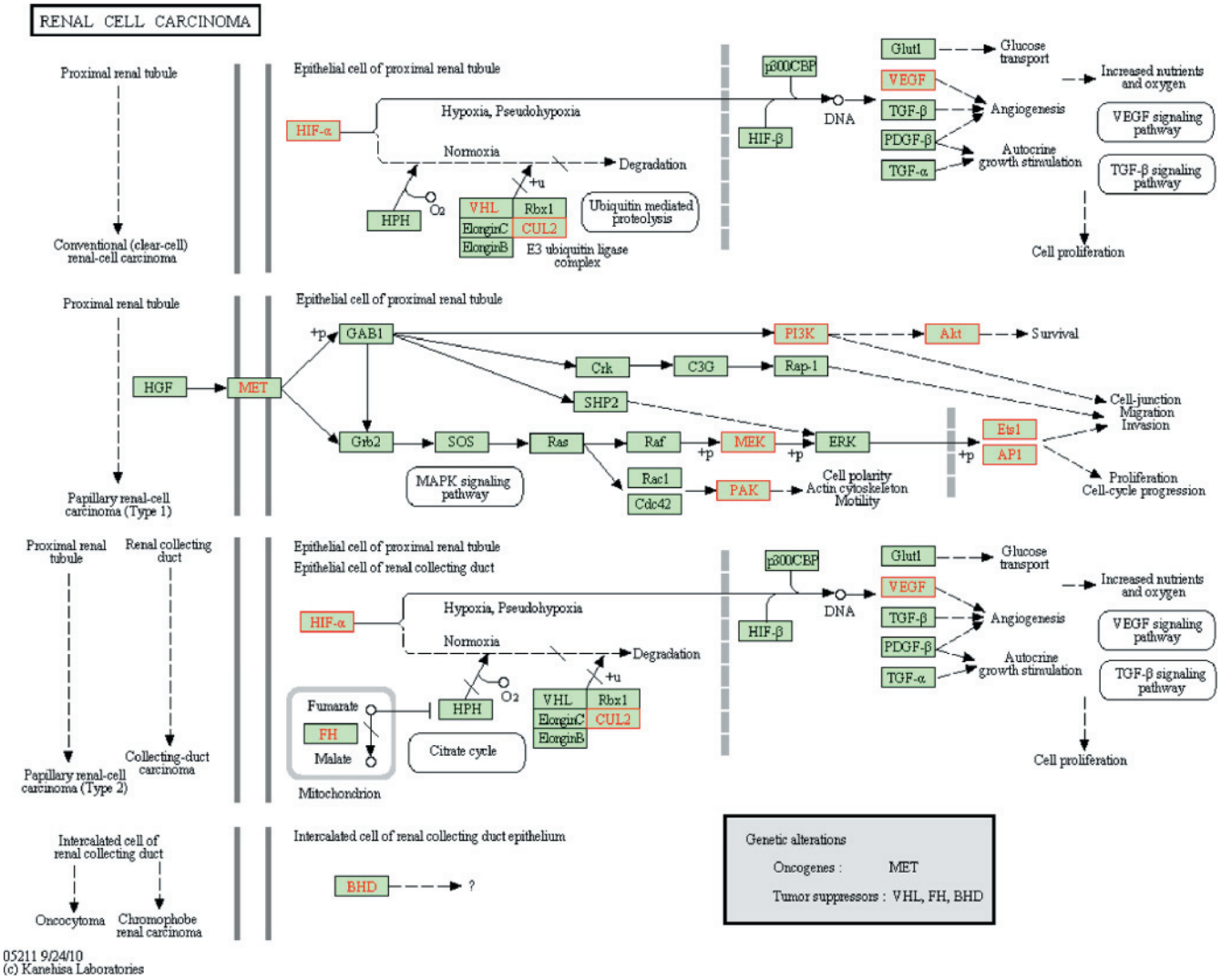

Figure W5. RCC pathway and prolonged response genes. Genes from KEGG RCC pathway targeted by miRNAs (red) included in prolonged response models.

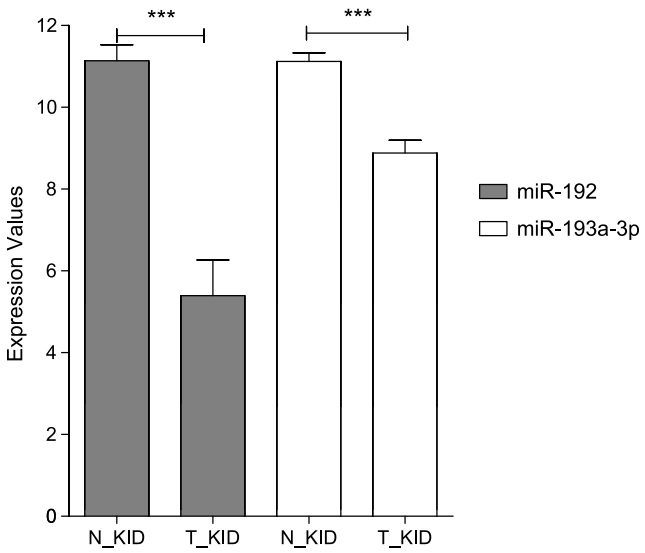

Figure W6. Expression of miRNAs in renal carcinomas. miR-192 and miR-193a-3p expression in normal (N_KID) and tumoral (T_KID) kidneys. ***$P < .001$. Data obtained from Lu et al.

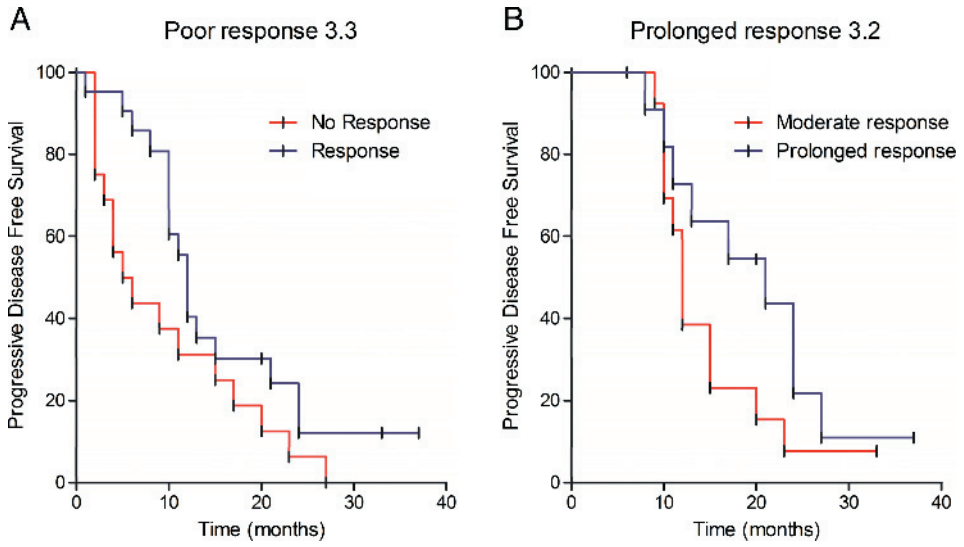

Figure W7. Validation of some predictive signatures using RT-qPCR. (A) Kaplan-Meier analyses of poor response model 3.3; HR between groups was 2.067 (IC95 = 0.97–4.39, $P = .059$). (B) Kaplan-Meier analyses of prolonged response model 3.2; HR between groups was 1.962 (IC95 = 0.77–4.96, $P = .155$).